



77-1-171

/nc

CERN/PS/LIN 76-7

4 November 1976

MONITORING OF PARTICLE BEAMS AT HIGH FREQUENCIES

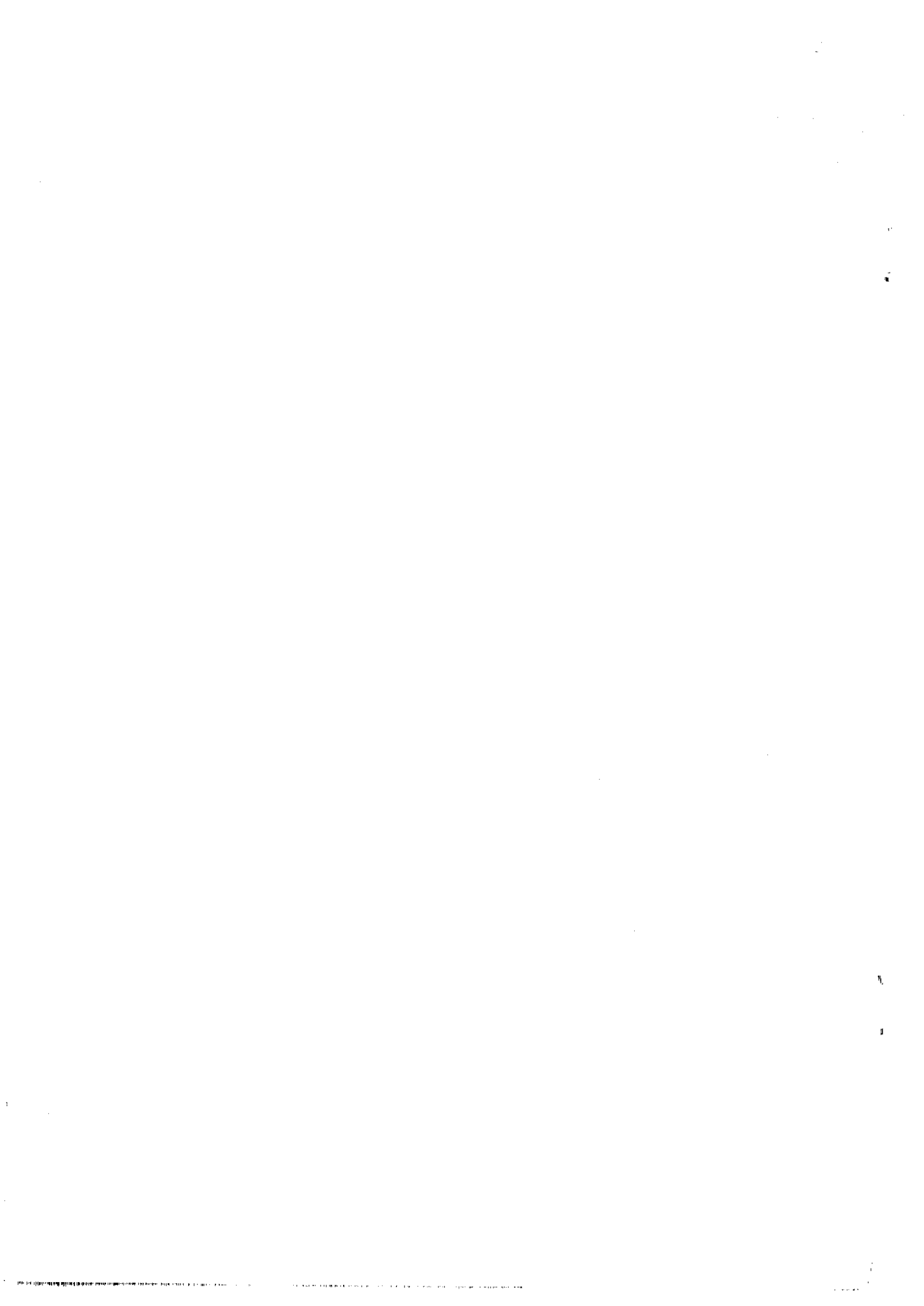
J. Cuperus

CERN - Geneva

A B S T R A C T

For a modulated beam, Green's function is often obtained by modulating Green's function for a uniform beam with the varying intensity of the beam. For a beam with high frequency modulation and low speed, this may not be accurate. More general formulas are presented and applied to electrostatic, wall-current, loop and stripline monitors. The response of 4-sector, 4-point and split-electrode position monitors is calculated. Finally, a very general reciprocity formula is presented.

Submitted to Nuclear Instruments and Methods.



I. FIELD OF THE BEAM IN A CYLINDRICAL BEAM PIPE

We consider a beam, moving in a cylindrical beam pipe with axis z (Fig. 1). Any curvature of the pipe in the z direction is neglected. In the plane perpendicular to the z axis, we use the curved orthogonal coordinates u, w , with $\bar{l}_u \times \bar{l}_w = \bar{l}_z$ and distance defined as :

$$dl^2 = e_1 du^2 + e_2 dw^2 + dz^2$$

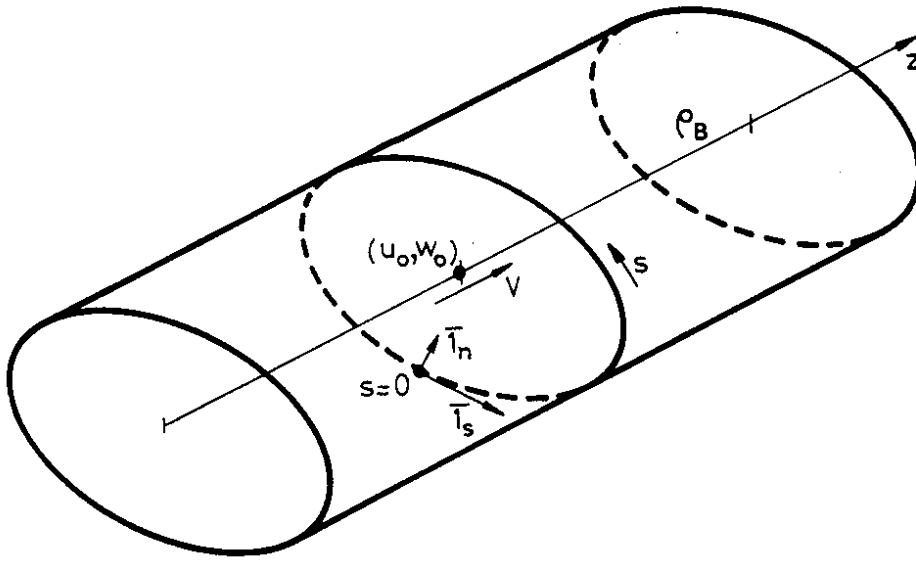


fig. 1 : The coordinate system in the beam pipe.

The particles in the beam move, with speed V , in the z direction. We suppose the beam is infinitely thin and going through (u_0, w_0) . We expand the charge of the beam in a Fourier series and study the field of each of the components separately.

The component with wavelength λ is given by :

$$\rho_B(\lambda, z) = D_\lambda \cdot \cos\left[\frac{2\pi}{\lambda}(V \cdot t + z_\lambda - z)\right] \frac{\delta(u-u_0) \cdot \delta(w-w_0)}{e_1 \cdot e_2} \quad (1)$$

ρ_B is the charge density of the Fourier component. D_λ is the amplitude, in Coulomb per meter, and $2\pi z_\lambda/\lambda$ is a phase angle.

We make a Lorentz transform to the reference system (u, w, z^*) where the beam is at rest :

$$z^* = \gamma \cdot (z - z_\lambda - V \cdot t) \quad (2)$$

$$\gamma = 1/\sqrt{1 - V^2/c^2}$$

$$\rho_B^*(\lambda, z^*) = \frac{D_\lambda}{\gamma} \cdot \cos\left(\frac{2\pi}{\gamma\lambda} \cdot z^*\right) \cdot \frac{\delta(u-u_0) \cdot \delta(w-w_0)}{e_1 \cdot e_2} \quad (3)$$

The transformed quantities are marked with an *. We suppose the wall perfectly conducting, so that the moving wall is at a uniform potential. In the new reference system, we have a pure electrostatic problem. The field ϕ^* is determined with :

$$\nabla^2 \Phi^*(u, w, z^*) = -\rho_B^*(\lambda, z)/\epsilon_0 \quad (4)$$

We look for a solution of the form

$$\Phi^* = F^*(u, w) \cdot \frac{D_\lambda}{\gamma} \cdot \cos\left(\frac{2\pi}{\gamma\lambda} \cdot z^*\right) \quad (5)$$

and, with (4) :

$$\nabla_{u,w}^2 F^* - \left(\frac{2\pi}{\gamma\lambda}\right)^2 \cdot F^* = -\frac{\delta(u-u_0) \cdot \delta(w-w_0)}{\epsilon_0 \cdot e_1 \cdot e_2} \quad (6)$$

If we can find a solution for (6), we know ϕ^* . Returning to the reference system (u, w, z) , where the beam pipe is at rest, we find :

$$E_u = -\gamma \cdot \frac{\partial \Phi^*}{\partial u} \quad , \quad E_w = -\gamma \cdot \frac{\partial \Phi^*}{\partial w} \quad , \quad E_z = -\frac{\partial \Phi^*}{\partial z^*} \quad (7)$$

The surface charge σ , induced on the wall, is :

$$\sigma(s, z) = \epsilon_0 \cdot E_n(o) \quad (8)$$

with $E_n(n)$ the field component perpendicular to the wall and s the co-ordinate on the circumference.

If the frequency is high enough, so that E.M. fields cannot penetrate the wall, we have

$$B_u = -\frac{V}{c^2} E_w \quad , \quad B_w = \frac{V}{c^2} E_u \quad , \quad B_z = 0 \quad (9)$$

The current flowing on the inside of the wall (in the z direction) is then :

$$i(s, z) = \frac{B_s}{\mu_0} = \frac{V}{\mu_0 c^2} E_n(o) = V \cdot \sigma(s, z) \quad (10)$$

with B_s the magnetic field close to the wall.

I.1 Rectangular cross-section

We work in rectangular co-ordinates x, y, z (Fig. 2)

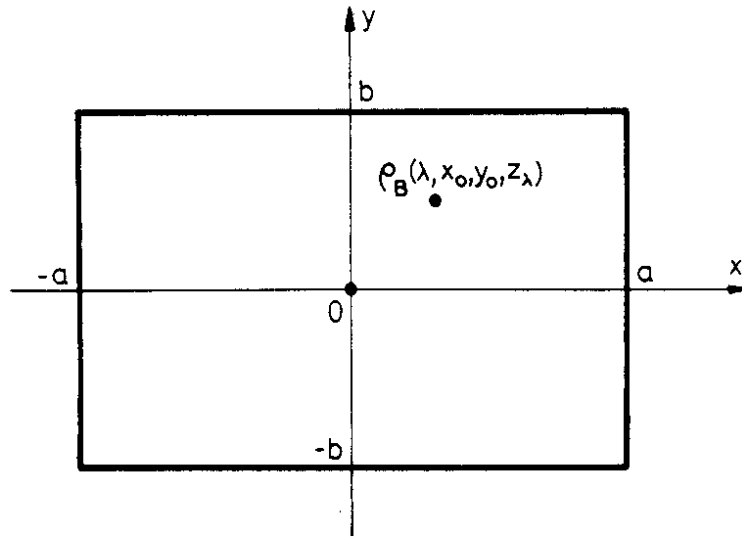


fig. 2 : Cross section of a rectangular beam pipe.

A solution of (6), valid for $y \ll y_0$ is :

$$F^*(x, y) = \sum_{m=1}^{\infty} \frac{\text{sh}[\alpha_m(b-y_0)] \cdot \text{sh}[\alpha_m(b+y)]}{\epsilon_0 \cdot a \cdot \alpha_m \cdot \text{sh}(2b \cdot \alpha_m)} \cdot \sin\left[\frac{m\pi(x_0+a)}{2a}\right] \cdot \sin\left[\frac{m\pi(x+a)}{2a}\right] \quad (11)$$

with
$$\alpha_m = \sqrt{\left(\frac{2\pi}{\lambda}\right)^2 + \left(\frac{m\pi}{2a}\right)^2}$$

And the surface charge, induced on the wall $y = -b$ is :

$$\sigma_{y=-b}(x,z) = -D_{\lambda} \cos\left[\frac{2\pi}{\lambda}(V.t + z_{\lambda} - z)\right] \cdot \sum_{m=1}^{\infty} \frac{\sin\left[\frac{m\pi(x+a)}{2a}\right] \cdot \text{sh}\left[\alpha_m(b-y_0)\right]}{a \cdot \text{sh}(2b \cdot \alpha_m)} \cdot \sin\left[\frac{m\pi(x+a)}{2a}\right] \quad (12)$$

By exchanging $-y_0$ for y_0 , we get the charge on the wall $y = b$ and, by exchanging (x, x_0, a) for (y, y_0, b) , we get the charge on the other two walls.

1.2 Circular cross-section

We work in cylindric co-ordinates r, ϕ, z (Fig. 3).

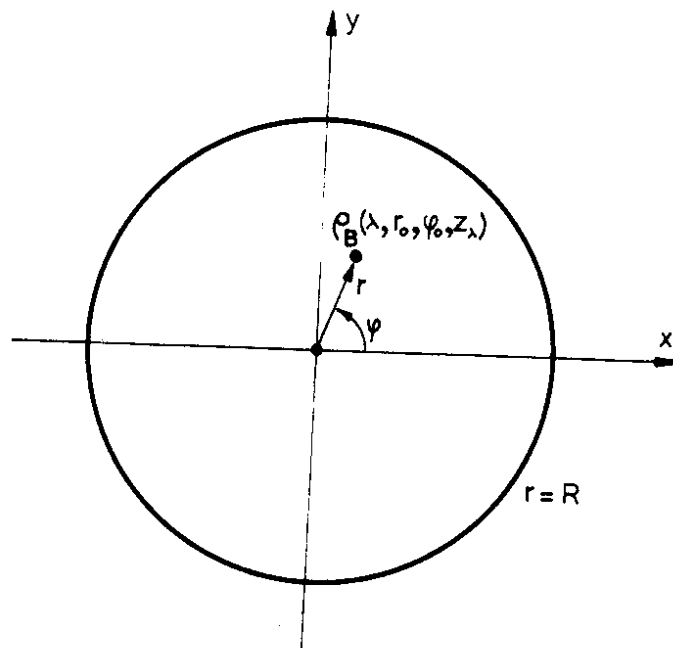


fig. 3 : Cross section of a circular beam pipe.

A solution of (6), valid for $r \gg r_0$, is :

$$F^*(z, \varphi) = - \sum_{m=0}^{\infty} \frac{I_m\left(g \frac{z_0}{R}\right)}{\epsilon_0 \cdot \pi \cdot N} \cdot \left[\frac{K_m(g)}{I_m(g)} \cdot I_m\left(g \frac{z}{R}\right) - K_m\left(g \frac{z}{R}\right) \right] \cdot \cos[m(\varphi - \varphi_0)] \quad (13)$$

with $g = 2HR / \gamma\lambda$, $N = 2$ for $m = 0$ and $N = 1$ for $m \geq 1$. The radial electric field is, again for $r \gg r_0$:

$$E_z(\tau, \varphi, z) = D_\lambda \cdot \cos\left[\frac{2\pi}{\lambda}(V.t + z_\lambda - z)\right] \cdot \sum_{m=0}^{\infty} \frac{g \cdot I_m\left(g \frac{z_0}{R}\right)}{\epsilon_0 \pi N R I_m(g)} \cdot \left[K_m(g) \cdot I'_m\left(g \frac{z}{R}\right) - K'_m\left(g \frac{z}{R}\right) \cdot I_m(g) \right] \cdot \cos[m(\varphi - \varphi_0)] \quad (14)$$

The charge induced on the wall is :

$$\sigma(\varphi, z) = -D_\lambda \cdot \cos\left[\frac{2\pi}{\lambda}(V.t + z_\lambda - z)\right] \cdot \sum_{m=0}^{\infty} \frac{1}{\pi N R} \cdot \frac{I_m\left(g \frac{z_0}{R}\right)}{I_m(g)} \cdot \cos[m(\varphi - \varphi_0)] \quad (15)$$

E_r , as given by (14) is not easy to calculate. Close to the wall we can use the approximate value :

$$E_z(\tau) \cong E_z(R) - \left[\frac{\partial E_z(\tau)}{\partial z} \right]_{z=R} \cdot (R - z) = \frac{2R - z}{R} \cdot E_z(R) \quad (16)$$

1.3 Longitudinal field

We can find the longitudinal electric field with (7). Here we will derive E_z from the transverse component E_n . Along the path 1,2,3,4,1 of Fig. 4, we have, with Δz small :

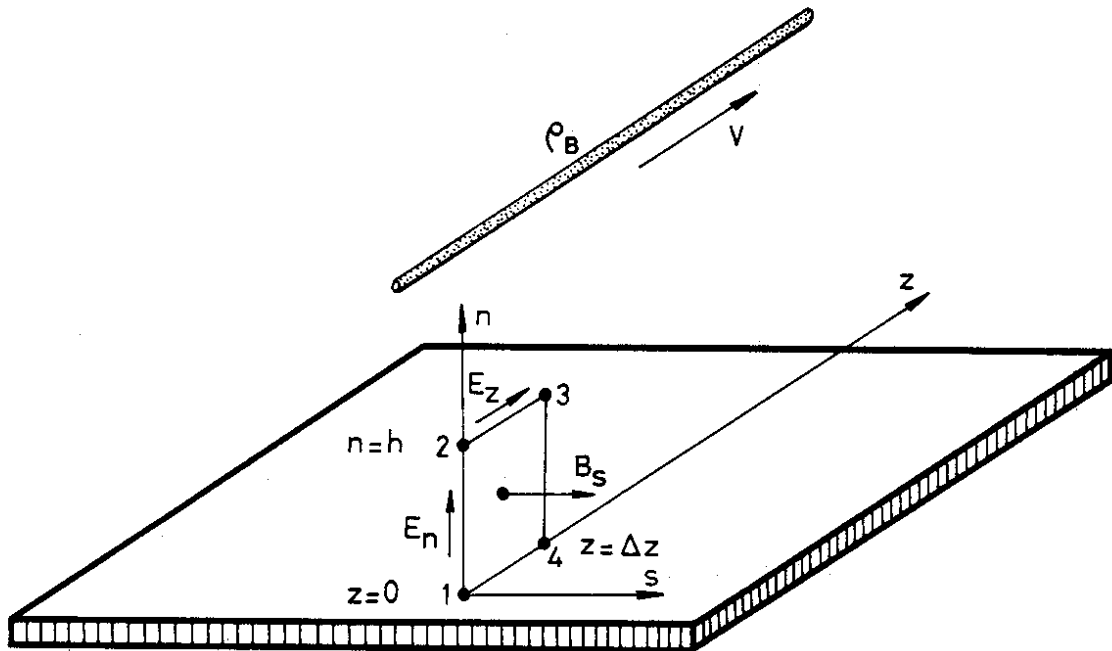


fig. 4 : Field at the wall of the beam pipe.

$$\int_0^h E_n(n) \cdot dn + E_z(h) \cdot \Delta z - \int_0^h \left[E_n(n) + \Delta z \frac{\partial E_n(n)}{\partial z} \right] \cdot dn = \Delta z \int_0^h \frac{\partial B_s(n)}{\partial t} \cdot dn$$

and, with $B_s(n)$ given by (9) :

$$E_z(h) = \left[\frac{\partial}{\partial z} + \frac{V}{c^2} \cdot \frac{\partial}{\partial t} \right] \cdot \int_0^h E_n(n) \cdot dn \quad (17)$$

In general, E_n is of the form :

$$E_n(n) = D_\lambda \cdot F(n, s) \cdot \cos \left[\frac{2\pi}{\lambda} (V \cdot t + z_\lambda - z) \right] \quad (18)$$

We then find, for E_z :

$$E_z(n) = D_\lambda \cdot \frac{2\pi}{\gamma^2 \lambda} \cdot G(n, s) \cdot \sin \left[\frac{2\pi}{\lambda} (V \cdot t + z_\lambda - z) \right] \quad (19)$$

with : $G_n(n, s) = \int_0^h F(n, s) \cdot dn \quad (20)$

II. COUPLING BETWEEN FIELD AND MONITOR

For an electrode, cut out of the wall, the charge induced is, of course, the integral of $\sigma(s, z)$ over the surface of the electrode. For a wall current monitor, the current flowing, through an impedance over a transverse gap, is the integral of $i(s, z)$ over the length of the gap, if we prevent the current from flowing around the gap. We will now discuss two less obvious couplings.

II.1 Stripline coupling

A stripline with impedance Z is mounted, in the z direction, on the wall of the beam pipe (Fig. 5). This coupling has been calculated by Kerns and Large¹⁾ (who also used Eq. 21) . The present treatment is somewhat simpler and more general.

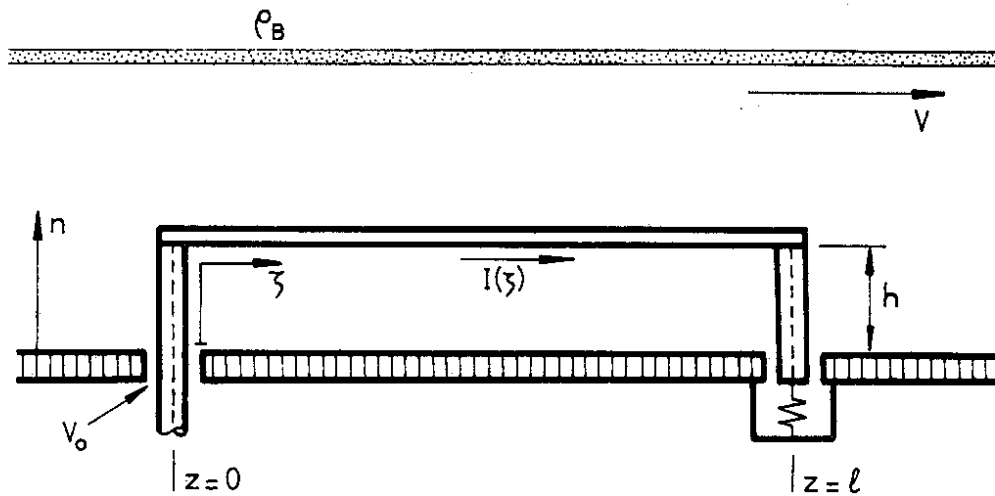


fig. 5 : Stripline coupling.

We use the $\exp(j\omega t)$ convention. The open-circuit voltage V_0 is given ²⁾ by :

$$V_0 = - \frac{1}{I_1} \int_v \bar{E}_0 \cdot \bar{J} \cdot dv \quad (21)$$

v is the inside of the beam pipe. \bar{E}_0 is the electric field due to the beam but with the stripline removed. \bar{J} is the current density over the line when the line is driven, at the open end, with a test current I_1 .

The line is terminated, at $z = l$, in its characteristic impedance. We suppose the strip is thin and at a uniform height h above the wall of the beam pipe (if the wall is curved, the strip is curved also). For $Z = 50$ or 75 Ohm, the strip is several times wider than h and the current is concentrated on the underside of the strip. We can replace \bar{J} by a line current $I(\zeta)$, going through the middle of the underside of the strip and through the center of the supporting posts. This test current is :

$$I_1 = 1 \quad , \quad I(\zeta) = e^{-j \frac{\omega}{c} \zeta} \quad , \quad \omega = \frac{2\pi}{\lambda} \cdot V$$

We suppose the components of the electric field known and of the form (18) and (19) :

$$E_n(n, z) = D_\lambda \cdot F(n) \cdot e^{j \frac{2\pi}{\lambda} (z_\lambda - z)}$$

$$E_z(n, z) = -j \frac{2\pi}{\gamma^2 \lambda} \cdot D_\lambda \cdot G(n) \cdot e^{j \frac{2\pi}{\lambda} (z_\lambda - z)}$$

For the calculation of (21), we make the following approximations :

$$\int_0^h e^{-j \frac{\omega}{c} n} \cdot F(n) \cdot dn \cong G(h) \cdot e^{-j \frac{\omega}{c} \cdot \frac{h}{2}}$$

$$\int_0^h e^{-j \frac{\omega}{c} (l+2h-n)} \cdot F(n) \cdot dn \cong G(h) \cdot e^{-j \frac{\omega}{c} (l + \frac{3}{2} h)}$$

$$1 - \frac{V}{c} - e^{\pm j \frac{\omega}{c} \cdot \frac{h}{2}} \cong -\frac{V}{c} e^{\pm j \frac{\pi h}{\lambda}}$$

After some simple calculations, we find :

$$V_0 = \frac{2V}{c} \cdot D_\lambda \cdot G(h) \cdot \sin \left[\frac{\pi}{\lambda} \left(l + \frac{V}{c} l + h \right) \right] \cdot e^{j \cdot \varphi_\lambda} \quad (22)$$

$$\varphi_\lambda = -\frac{\pi}{2} + \frac{2\pi}{\lambda} \left[z_\lambda - \frac{l}{2} - \frac{V}{c} \left(\frac{l}{2} + h \right) \right]$$

For $V = -c$, V_0 is almost zero. For $V = c$, the response is maximum for $l \cong \lambda/4$. Due to several approximations, the accuracy of (22) will probably not be better than $\pm 5\%$. Usually, however, the absolute response is not so important. What is important, for position measurement, is that V_0 is proportional to $G(h)$.

II.2 Loop coupling

The loop is mounted on the wall of the beam pipe (Fig. 6).

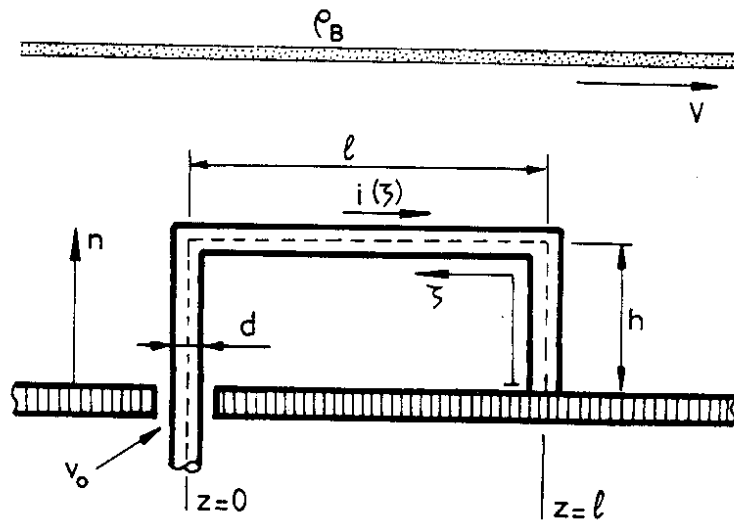


fig. 6 : Loop coupling.

We use the same method as for the stripline. Now, we suppose \bar{J} to be uniformly distributed over the surface of the wire, for each value of ζ (this is not exactly true : the current has a tendency to concentrate on the underside of the wire but, for $h \gg d$, the approximation is good). We can replace \bar{J} by $i(\zeta)$ through the center of the wire. $i(\zeta)$ is now a standing wave and we have, approximately :

$$i(\zeta) = \cos(\omega t) \cdot \cos\left(\frac{\omega \zeta}{c}\right)$$

$$i_1 = i(\ell + 2h) = \cos(\omega t) \cdot \cos\left[\frac{\omega}{c}(\ell + 2h)\right]$$

The integral (21) reduces to a line integral over the center of the wire. With E_n and E_z of the form (18) and (19) and the same approximations as before, for the integrals of $F(n)$, but now with the \cos function, we find :

$$v_0 = \frac{V}{c} \cdot \frac{D_\lambda \cdot G(h)}{\cos\left[\frac{\omega}{c}(\ell + 2h)\right]} \left\{ A \cdot \sin\left[\frac{2\pi}{\lambda}(V \cdot t + z_\lambda)\right] + B \cdot \cos\left[\frac{2\pi}{\lambda}(V \cdot t + z_\lambda)\right] \right\} \quad (23)$$

$$A = \sin\left[\frac{\omega}{c}(h + \ell)\right] - \sin\left(\frac{\omega}{c}h\right) \cdot \cos\left(\frac{2\pi\ell}{\lambda}\right)$$

$$B = \sin\left(\frac{\omega}{c}h\right) \cdot \sin\left(\frac{2\pi\ell}{\lambda}\right) - \frac{\pi h}{\lambda} \cdot \sin\left[\frac{\omega}{c}\left(\ell + \frac{5h}{4}\right)\right]$$

Usually, B is much smaller than A . Only $G(h)$ varies with the beam position and v_0 is again proportional to $G(h)$. With h and ℓ much smaller than λ , (23) reduces, of course, to Faraday's law.

The impedance of the loop depends on ℓ , h and d . A few values, valid for small dimensions of the loop, are given in ³⁾. For more precision, it is better to measure the impedance on the finished monitor.

III. INTENSITY MONITORS

For intensity measurements of the beam, we can either detect the D.C. component (in fact usually varying in time) or the fundamental Fourier component. When the beam is tightly bunched by the accelerating R.F. field, this fundamental component is almost independent of the exact shape and width of the bunches. Measurement of the fundamental component can be an advantage for eliminating the effect of stray particles and noise and also for obtaining a higher sensitivity or for a better response to low frequency modulation. When we want to look at the shape of the bunches, we are also interested in the higher harmonics.

III.1 Rectangular electrostatic monitor

For an electrode, mounted flush with the wall, with length L centered on $z = 0$ and rectangular cross-section $2a \times 2b$ (Fig. 2), the charge q , induced by the Fourier component of the beam with wavelength λ , is the integral of σ over the surface of the electrode. With (12) and similar formulas for the other three sides, we find :

$$q = -D_\lambda \cdot \cos\left[\frac{2\pi}{\lambda}(V.t + z_\lambda)\right] \cdot \frac{\sin(\pi L/\lambda)}{\pi/\lambda} \cdot \eta(\gamma\lambda, x_0, y_0) \quad (24)$$

$$\eta = \sum_{m=1,3,\dots}^{\infty} \frac{4}{m\pi} \left\{ \sin\left[\frac{m\pi(x_0+a)}{2a}\right] \cdot \frac{\text{ch}(\alpha_m y_0)}{\text{ch}(\alpha_m b)} + \sin\left[\frac{m\pi(y_0+b)}{2b}\right] \cdot \frac{\text{ch}(\beta_m x_0)}{\text{ch}(\beta_m a)} \right\}$$

$$\alpha_m = \sqrt{\left(\frac{2\pi}{\lambda}\right)^2 + \left(\frac{m\pi}{2a}\right)^2}, \quad \beta_m = \sqrt{\left(\frac{2\pi}{\lambda}\right)^2 + \left(\frac{m\pi}{2b}\right)^2}$$

η is a correction factor, close to 1 if $\gamma\lambda$ is large with respect to $2a$ and $2b$ (and always 1 for a beam close to the wall). For a centered beam :

$$\eta(\gamma\lambda, 0, 0) = \sum_{m=1,3,\dots}^{\infty} \frac{4 \sin\left(\frac{m\pi}{2}\right)}{m\pi} \left[\frac{1}{\text{ch}(\alpha_m b)} + \frac{1}{\text{ch}(\beta_m a)} \right] \quad (25)$$

III.2 Circular electrostatic monitor

We consider now an electrode with a circular cross section of radius R (Fig. 3). The electrode is again of length L , centered on $z = 0$. The charge q , induced on the electrode is, with σ given by (15) :

$$q = -D_\lambda \cdot \cos\left[\frac{2\pi}{\lambda}(V.t + z_\lambda)\right] \cdot \frac{\sin(\pi L/\lambda)}{\pi/\lambda} \cdot \frac{I_0(g r_0/R)}{I_0(g)} \quad (26)$$

The high frequency response is limited by the length L of the electrode. It is also limited by the Bessel factor. The Bessel factor, for a centered beam, is down to 0.7 (-3dB) for $g \cong 1.2$ or $\gamma\lambda \cong 5R$.

We now calculate the response to a diffuse beam. We limit ourselves to a centered beam with radius r_1 and charge density ρ_B constant over the cross-section (Fig. 7). We have then

$$\rho_B = \frac{D_\lambda}{\pi \cdot r_1^2} \cdot \cos\left[\frac{2\pi}{\lambda}(V.t + z_\lambda - z)\right] \quad z \leq r_1$$

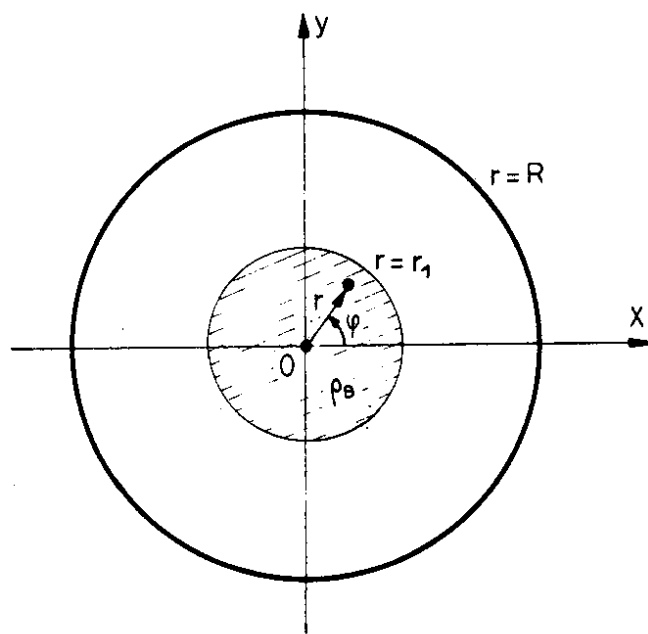


fig. 7 : Diffuse beam.

The charge, induced on the electrode, is then, by integration of (26) over the cross-section of the beam :

$$q = -D_{\lambda} \cdot \cos \left[\frac{2\pi}{\lambda} (V \cdot t + z_{\lambda}) \right] \cdot \frac{\sin(\pi L / \lambda)}{\pi / \lambda} \cdot \frac{1}{I_0(g)} \cdot \frac{2 I_1(g z_1 / R)}{g z_1 / R} \quad (27)$$

We will illustrate this with the example of the 30 MeV output of a 200 MHz proton linac. We measure the intensity with a circular pick-up with $R = 30$ mm. The parameters are : $\beta = 0.314$, $\gamma = 1.05$, $\lambda = 472$ mm, $\gamma\lambda/R = 16.6$, $g = 0.380$. The correction factor for a centered pencil beam is then :

$$\eta_1 = 1 / I_0(g) = 0.965$$

For a diffuse beam with $r_1 = 20$ mm this is :

$$\eta_2 = \eta_1 \cdot \frac{2 I_1(g z_1 / R)}{g z_1 / R} = 0.973$$

For a pencil beam, 10 mm off center, this is :

$$\eta_3 = \eta_1 \cdot I_0(g z_0 / R) = 0.969$$

Precise measurements are still possible if we correct for η_1 . This occurs automatically when we calibrate the monitor against a more absolute one. The response to higher harmonics is limited, however, and measurement of the bunch form is not possible.

III.3 Elliptical electrostatic monitor

The solution of (6) for the elliptical cross-section, leads to Mathieu functions which are difficult to calculate. A good approximation for the response can be obtained by comparing the results for the square and the circular monitor. For different values of g and a beam not too close to the wall, (24) and (26) give almost the same result if we take $a = 0.92R$. We can extend this result to elliptical monitors : the response of the elliptical monitor should be very similar to that of a rectangular monitor with a and b 0.92 times the half-axes of the ellipse.

III.4 Wall current monitor

In a wall current intensity monitor, the wall is cut at $z = 0$. The total current i that would normally flow over the inside of the wall, is deviated over an external circuit where it is measured (Avery et Al. ⁴). For a circular cross-section, with radius R :

$$i = \int_0^{2\pi} R.V. \sigma(\varphi, z | z_0, \varphi_0, z_\lambda). d\varphi$$

and, with σ given by (15) :

$$i = -V.D_\lambda. \cos\left[\frac{2\pi}{\lambda}(V.t + z_\lambda)\right]. \frac{I_0(gz_0/V)}{I_0(g)} \quad (28)$$

All the formulas obtained for the electrostatic monitor are valid, if we replace $\sin(\pi L/\lambda)/(\pi/\lambda)$ by V .

IV. FOUR SECTOR MEASUREMENTS

We limit ourselves to circular cross-sections (Fig. 8). The calculations will be made for a wall current monitor (at $z = 0$) but they are also valid, with small changes, for an electrostatic electrode, cut into four pieces.

We measure separately the currents i_1 to i_4 , through the four sectors. The sum signal is given by (28) :

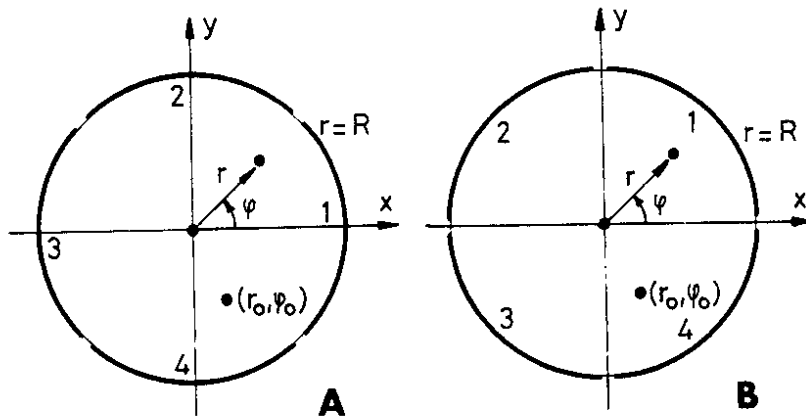


fig. 8 : Two configurations for a four sector monitor.

$$S = i_1 + i_2 + i_3 + i_4 = H \cdot \frac{I_0(g \xi_0/R)}{I_0(g)}$$

$$H = -V \cdot D_\lambda \cdot \cos \left[\frac{2\pi}{\lambda} (V \cdot t + z_\lambda) \right]$$

The difference signals, for the cases A and B, are :

$$\Delta_A = i_1 - i_3 = \frac{4H}{\pi} \sum_{m=1,3,\dots}^{\infty} \frac{I_m(g \xi_0/R)}{m \cdot I_m(g)} \cdot \cos(m\varphi_0) \cdot \sin\left(\frac{m\pi}{4}\right) \quad (29)$$

$$\Delta_B = (i_1 + i_4) - (i_2 + i_3) = \frac{4H}{\pi} \sum_{m=1,3,\dots}^{\infty} \frac{I_m(g \xi_0/R)}{m \cdot I_m(g)} \cdot \cos(m\varphi_0) \cdot \sin\left(\frac{m\pi}{2}\right) \quad (30)$$

For $g \leq 1.2$ (or $\gamma\lambda \geq 5R$), we can approximate I_3 and higher by the first term of their series expansion. We find :

$$P_{xA} = \frac{\pi R}{\sqrt{8}} \cdot \frac{\Delta_A}{S} = R \cdot \frac{I_0(g)}{I_0(g \xi_0/R)} \left[\frac{I_1(g \xi_0/R)}{I_1(g)} \cdot \cos(\varphi_0) + \frac{1}{3} \left(\frac{\xi_0}{R}\right)^3 \cos(3\varphi_0) - \frac{1}{5} \left(\frac{\xi_0}{R}\right)^5 \cos(5\varphi_0) - \dots \right] \quad (31)$$

$$P_{xB} = \frac{\pi R}{4} \cdot \frac{\Delta_B}{S} = R \cdot \frac{I_0(g)}{I_0(g \xi_0/R)} \left[\frac{I_1(g \xi_0/R)}{I_1(g)} \cdot \cos(\varphi_0) - \frac{1}{3} \left(\frac{\xi_0}{R}\right)^3 \cos(3\varphi_0) + \frac{1}{5} \left(\frac{\xi_0}{R}\right)^5 \cos(5\varphi_0) - \dots \right] \quad (32)$$

P_x is a good measure for $x_0 = r_0 \cos(\varphi_0)$ when $r_0 \leq 0.5R$ and $\gamma\lambda \geq 5R$. Measurement of the y_0 co-ordinate leads, of course, to the same formulas.

V. FOUR POINT MEASUREMENTS

We limit ourselves again to the circular cross-section.

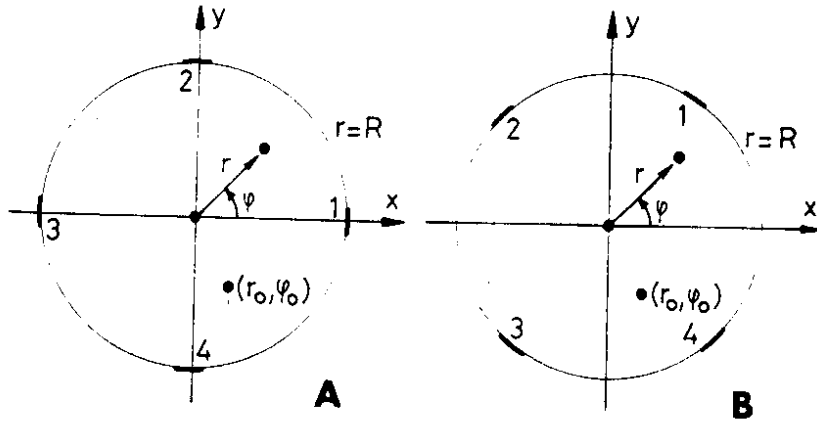


fig. 9 : Two configurations for a four point monitor.

We will study the configuration of Fig. 9, first for four small electrodes, each with surface T , cut out of the wall. We suppose, approximatively, that the charge density σ is constant over the surface of the electrodes and equal to σ in the center. The sum, S_A , of the charges on the four electrodes, for configuration A, is then, with (15) :

$$S_A = q_1 + q_2 + q_3 + q_4 = 4H \cdot \sum_{m=0,4,8,\dots}^{\infty} \cos(m\varphi_0) \frac{I_m(gz_0/R)}{H\pi R I_m(g)} \quad (33)$$

$$H = -D_\lambda \cdot T \cdot \cos\left[\frac{2\pi}{\lambda}(V \cdot t + z_\lambda)\right]$$

For the difference term, we find :

$$\Delta_A = q_1 - q_3 = \frac{2H}{\pi R} \cdot \sum_{m=1,3,\dots}^{\infty} \cos(m\varphi_0) \cdot \frac{I_m(gz_0/R)}{I_m(g)} \quad (34)$$

and, for $\gamma\lambda \gg 5R$ and $r_0 \leq 0.5R$, we can measure the position with :

$$P_{XA} = R \frac{\Delta_A}{S_A} = R \frac{\frac{I_1(gz_0/R)}{I_1(g)} \cdot \cos(\varphi_0) + \left(\frac{z_0}{R}\right)^3 \cos(3\varphi_0) + \left(\frac{z_0}{R}\right)^5 \cos(5\varphi_0) + \dots}{\frac{I_0(gz_0/R)}{I_0(g)} + 2\left(\frac{z_0}{R}\right)^4 \cdot \cos(4\varphi_0) + \dots} \quad (35)$$

For the configuration B, we have :

$$S_B(R, \tau_0, \varphi_0) = S_A(R, \tau_0, \varphi_0 + \frac{\pi}{4})$$

$$\Delta_B = (q_1 + q_4) - (q_2 + q_3)$$

$$P_{XB} = \frac{R}{\sqrt{2}} \cdot \frac{\Delta_B}{S_B} = R \frac{\frac{I_1(g\tau_0/R) \cos(\varphi_0) - \left(\frac{\tau_0}{R}\right)^3 \cos(3\varphi_0) - \left(\frac{\tau_0}{R}\right)^5 \cos(5\varphi_0) + \dots}{\frac{I_0(g\tau_0/R)}{I_0(g)} - 2\left(\frac{\tau_0}{R}\right)^4 \cos(4\varphi_0) + \dots}}{\quad} \quad (36)$$

V.1 Four loops or striplines

The open-circuit voltage, for a loop or stripline, at position ψ_1 , is :

$$V_0 = H \cdot G(h) = - \frac{H}{D_\lambda \cdot \cos\left[\frac{2\pi}{\lambda}(V \cdot t + z_\lambda - z)\right]} \int_{R-h}^R E_z(\tau, \varphi_1) \cdot d\tau$$

with H given by (22) for the stripline and (23) for the loop. With (16) and (14), we can find an approximate value for V_0 . An accurate calculation of a few limiting cases shows, however, that a better approximation can be obtained with a slightly different formula :

$$V_0 = -H \cdot \frac{h}{\epsilon_0 \cdot \pi (R - 0.5h)} \cdot \sum_{m=0}^{\infty} \cos[m(\psi_1 - \varphi_0)] \frac{I_m(g\tau_0/R^*)}{N \cdot I_m(g)} \quad (37)$$

with $R^* = R - 0.15h$. The sum, S_A , of the four voltages, for case A, is then :

$$S_A(\varphi_0) = -4H \frac{h}{\epsilon_0 \pi (R - 0.5h)} \cdot \sum_{m=0,4,8,\dots}^{\infty} \cos(m\varphi_0) \frac{I_m(g\tau_0/R^*)}{N \cdot I_m(g)} \quad (38)$$

We have again $S_B(\psi_0) = S_A(\psi_0 + \pi/4)$. The position of the beam is again given by (35) or (36), where we substitute R^* for R .

VI. SPLIT ELECTRODE PICK-UP

By far the most popular position monitor is the split electrode pick-up, of which Fig. 10 gives an example. We measure $P_x = (S_1 - S_2) / (S_1 + S_2)$, where S_1 and S_2 are signals, linearly related to the charges q_1 and q_2 induced on the electrodes by the beam. It was proved by Sherwood⁵⁾ that, for

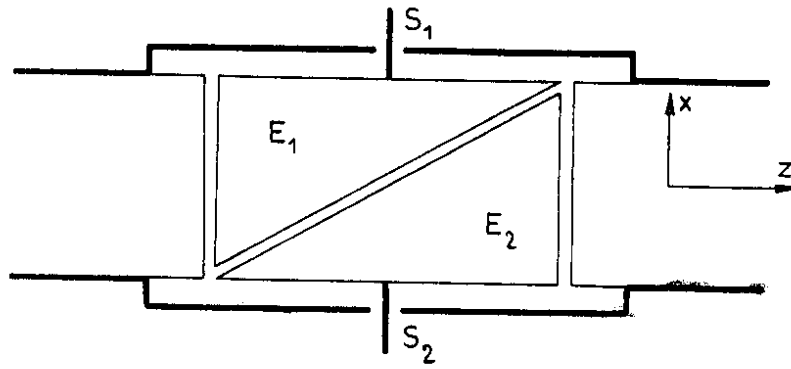


fig.10 : Top view of a split-electrode monitor.

electrodes cut out of the wall by planes parallel to the y axis, P_x is linearly related to the co-ordinate x_0 of the beam and independent of y_0 . This is valid for a cylindrical beam pipe of any cross-section and a beam, uniform in the z direction, over a length, large with respect to the electrode dimensions. We shall study here what happens when the beam is varying rapidly in the z direction.

The electrodes are separated by a gap. The charge, which would have fallen on the gap, is divided equally over the two electrodes and, for the purpose of calculating the induced charge, we can think of the electrodes as extending to the middle of the gap.

VI.1 Differential equation for q

The Fourier component of the beam is given by (1), with u and w replaced by x and y . (6) can now be written as :

$$\mathcal{L} \epsilon_0 F^*(x, y | x_0, y_0) = -\delta(x-x_0) \cdot \delta(y-y_0)$$

$$\mathcal{L} = \nabla_{x,y}^2 - \left(\frac{2\pi}{\gamma\lambda}\right)^2$$

The operator \mathcal{L} , together with the border condition $F^* = 0$, defines a self-adjoint problem. We have then, because of reciprocity :

$$\mathcal{L}_0 \epsilon_0 F^*(x, y | x_0, y_0) = -\delta(x-x_0) \cdot \delta(y-y_0) \quad (39)$$

$$\mathcal{L}_0 = \nabla_{x_0, y_0}^2 - \left(\frac{2\pi}{\gamma\lambda}\right)^2 \quad (40)$$

and, because of (5), we have :

$$\mathcal{L}_0 \epsilon_0 \Phi^*(x, y, z^* | x_0, y_0, z_\lambda^*) = -\delta(x-x_0) \cdot \delta(y-y_0) \cdot \frac{D_\lambda}{\gamma} \cdot \cos\left(\frac{2\pi}{\gamma\lambda} z^*\right) \quad (41)$$

Each instant t , we can calculate q_E , induced on the (moving) electrode (we suppose the electrode to be at ground potential) :

$$q_E = -\epsilon_0 \int_{S^*} \frac{\partial}{\partial n} [\Phi^*(x, y, z^* | x_0, y_0, z_\lambda^*)] dS^* \quad (42)$$

with S^* the transformed surface of the electrode. We let \mathcal{L}_0 operate on both sides of (42). \mathcal{L}_0 can be brought under the integral sign and, with (41) we find :

$$\mathcal{L}_0 q_E = 0 \quad (43)$$

q_E , as well as the co-ordinates x and y , are invariant under the Lorentz transformation. We conclude that (43) is also valid in the reference system where the beam pipe is stationary.

If we wish that q_E is only a function of x_0 and not of y_0 , we find as the solution of (43) :

$$q_E = A \cdot e^{+2\pi x_0 / \gamma \lambda} + B e^{-2\pi x_0 / \gamma \lambda} \quad (44)$$

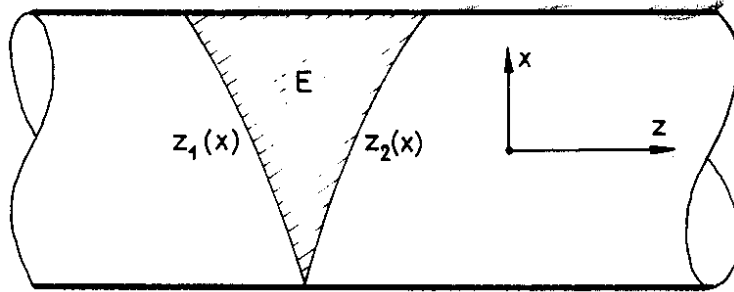


fig.11 : Shape of the electrode for linear response.

The response will be linear only when $\gamma \lambda$ is much larger than the transverse dimensions of the beam pipe. We now look for a border condition which matches (44). In Fig. 11, the electrode is defined by the cuts $z_1(x)$ and $z_2(x)$. When the beam approaches the wall, we have the border condition :

$$q_{EW}(x_0) = - \int_{z_1(x_0)}^{z_2(x_0)} \left[\iint \rho_B(\lambda, z) dx \cdot dy \right] dz \quad (45)$$

$$= - \frac{\lambda \cdot D_\lambda}{\pi} \cdot \cos \left[\frac{2\pi}{\lambda} (V \cdot t + z_\lambda - \frac{z_1 + z_2}{2}) \right] \cdot \sin \left(\frac{2\pi}{\lambda} \cdot \frac{z_2 - z_1}{2} \right) \quad (46)$$

(46) can be a border condition for (44) if :

$$z_1(x) + z_2(x) = 2z_0$$

$$\sin \left[\frac{2\pi}{\lambda} \cdot \frac{z_2(x) - z_1(x)}{2} \right] = C \cdot \operatorname{sh} \left(2\pi \cdot \frac{x + x_1}{\gamma \lambda} \right)$$

with z_0 , C and x_1 arbitrary constants. This allows us to calculate $z_1(x)$ and $z_2(x)$. We will not pursue this further because the cuts are usually linear and the question is then : what are the deviations from the linear response ?

VI.2 Electrode response for straight cuts

We will restrict ourselves to the "standard" configuration of Fig. 12 but the discussion can be easily adapted to other configurations. The border condition (46) is now, for electrode A :

$$q_{AW}(x_0) = - \frac{\lambda \cdot D_\lambda}{\pi} \cdot \cos \left[\frac{2\pi}{\lambda} \left(V \cdot t + z_\lambda - \frac{L}{2} \cdot \frac{x_0 + a}{2a} \right) \right] \cdot \sin \left(\frac{2\pi}{\lambda} \cdot \frac{L}{2} \cdot \frac{x_0 + a}{2a} \right) \quad (47)$$

We can write this as :

$$q_{AW} = - \frac{\lambda \cdot D_\lambda}{\pi} \left\{ \cos \left[\frac{2\pi}{\lambda} (V \cdot t + z_\lambda) \right] \cdot q_{wC}(x_0) + \sin \left[\frac{2\pi}{\lambda} (V \cdot t + z_\lambda) \right] \cdot q_{wS}(x_0) \right\} \quad (48)$$

$$q_{wC} = \cos \left(\frac{\pi L}{\lambda} \cdot \frac{x_0 + a}{2a} \right) \cdot \sin \left(\frac{\pi L}{\lambda} \cdot \frac{x_0 + a}{2a} \right)$$

$$q_{wS} = \sin^2 \left(\frac{\pi L}{\lambda} \cdot \frac{x_0 + a}{2a} \right)$$

With (48) as border condition and differential equation (43), we find $q_A(x_0, y_0)$ for all beam positions :

$$q_A(x_0, y_0) = - \frac{\lambda \cdot D_\lambda}{\pi} \left\{ \cos \left[\frac{2\pi}{\lambda} (V \cdot t + z_\lambda) \right] \cdot q_c(x_0, y_0) + \sin \left[\frac{2\pi}{\lambda} (V \cdot t + z_\lambda) \right] \cdot q_s(x_0, y_0) \right\} \quad (49)$$

with q_c and q_s the solutions of (43) with border conditions q_{wC} and q_{wS} .

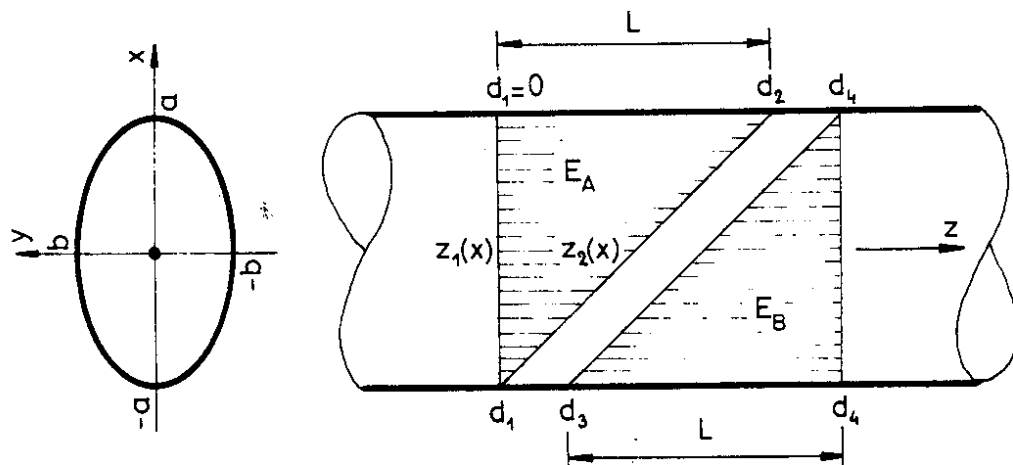


fig. 12: "Standard" electrode configuration for a split-electrode monitor.

We will measure the position with :

$$P_x(x_0, y_0) = \frac{Q_A - Q_B}{Q_A + Q_B} \cdot a \quad (50)$$

with Q_A the amplitude of q_A :

$$Q_A(x_0, y_0) = \frac{\lambda \cdot D_\lambda}{\pi} \sqrt{q_c^2(x_0, y_0) + q_s^2(x_0, y_0)} \quad (51)$$

To obtain q_c and q_s we write (43) as a difference equation :

$$\frac{q_1 + q_2 - 2q_0}{\Delta x^2} + \frac{q_3 + q_4 - 2q_0}{\Delta y^2} - \left(\frac{2\pi}{\delta\lambda}\right)^2 q_0 = 0 \quad (52)$$

We compute, with a relaxation method, consecutive values of q_0 out of the surrounding values q_1 to q_4 . Δx and Δy are the steps of the grid.

For the rectangular cross-section there are no problems.

The circle can be approximated by an octagon with all the corners on grid points. With $\Delta x \neq \Delta y$ this becomes an ellipse. A coarse grid is sufficient.

VI.3 Errors for the rectangular cross-section

We will pursue the calculation further for the rectangular cross-section $2a \times 2b$. When we measure with (50), three points are always exactly calibrated : the two end points, where $P_x(\pm a, y_0) = \pm a$ and the center where $P_x(0, y_0) = 0$ because of symmetry. With the beam close to the wall we find also, with (47) and (50) :

$$P_x(x_0, \pm b) = \cotg\left(\frac{\pi L}{2\lambda}\right) \cdot \tg\left(\frac{\pi L}{2\lambda} \cdot \frac{x_0}{a}\right) \cdot a \quad (53)$$

To get an idea about $P_x(x_0, y_0)$, we will compute the scale factor

$$P'_x(0, y_0) = \left[\frac{d P_x(x_0, y_0)}{d x_0} \right]_{x_0=0} \quad (54)$$

From (53), we get :

$$P'_x(0, \pm b) = \left(\frac{\pi L}{2\lambda}\right) \cdot \cotg\left(\frac{\pi L}{2\lambda}\right)$$

$P'_x(0,0)$ was computed on a grid of 7x7 internal points, for several values of γ and λ . The results are summarised in Table 1. We see that the difference in scale factor, between the wall and the center, is largest for λ small and $\gamma = 1$.

	γ	λ / L				
		3	4	5	7	10
$P'_x(0,b)$	-	0.91	0.95	0.97	0.98	0.99
$P'_x(0,0)$ $a=2b=L$	1	1.03	1.04	1.03	1.02	1.01
	2	0.96	0.98	0.99	0.99	1.00
	5	0.93	0.96	0.98	0.99	0.99
$P'_x(0,0)$ $2a=2b=L$	1	1.20	1.12	1.08	1.04	1.02
	2	1.03	1.02	1.01	1.00	1.00
	5	0.98	0.99	0.99	1.00	1.00
$P'_x(0,0)$ $2a=b=L$	1	1.46	1.27	1.18	1.09	1.04
	2	1.12	1.07	1.04	1.02	1.01
	5	1.02	1.01	1.00	1.00	1.00

table 1: Scale factor P'_x , for the position measurement, at the center and near the wall, for rectangular cross sections and different values of γ and λ .

VI.4 Diffuse beam

When we measure the position of a diffuse beam with a linear position monitor, we measure the center of charge of the charge distribution. This is still approximatively true when the deviations from linearity are not too large over the region covered by the beam. This remark is, of course, valid for all the position monitors considered here.

VII. RECIPROCITY

In some cases, the action of the beam on the monitor is difficult to calculate. Sometimes, the inverse problem turns out to be easier. Therefore, we will apply the general reciprocity formulas of Rumsey²⁾ to beam monitors. These formulas are valid, at any single frequency, for any passive linear system, even those containing anisotropic materials, but with the exception of gyrotropic media. We find, using the $\exp(j\omega t)$ convention :

$$V_o = - \frac{1}{I_1} \int \bar{J}_B(x, y, z) \cdot \bar{E}_1(x, y, z) \cdot dx \cdot dy \cdot dz \quad (55)$$

\bar{J}_B is the beam current density. \bar{E}_1 is the field in the monitor, without beam, due to a current source I_1 applied at the output. V_o is the open-circuit voltage, at the output, due to the beam but with I_1 removed. The integral is over the region where \bar{E}_1 is important.

Instead of a test current I_1 , we can apply a voltage source V_1 , at the output. The short-circuit current I_o , at the output, due to the beam but with V_1 removed, is then (I and V are positive in the same direction) :

$$I_o = \frac{1}{V_1} \int \bar{J}_B \cdot \bar{E}_1 \cdot dx \cdot dy \cdot dz \quad (56)$$

These formulas could be of use for calculating microwave monitors (e.g. Ref. 6) and also for magnetic monitors (e.g. Refs. 7, 8). For magnetic monitors, $\bar{E}_1 = -j\omega\bar{A}_1$ with \bar{A}_1 the magnetic potential.

REFERENCES

- 1) Q.A. Kerns and D.B. Large, Lawrence Berkeley Laboratory report, UCRL-11551 (July 1964).
- 2) V.H. Rumsey, IEEE Trans.Ant. and Prop. AP-11 (1963) 73.
- 3) H. Meinke and F.W. Grundlach, Taschenbuch der Hochfrequenz Technik (Springer-Verlag, 1968) p. 463.
- 4) R.T. Avery, A. Faltens and E.C. Hartwig, IEEE Trans.Nucl.Sci. NS-18 (1971) 920.
- 5) A.J. Sherwood, IEEE Trans.Nucl.Sci. NS-12 (1965), 925.
- 6) Farinholt et al., IEEE Trans.Nucl.Sci. NS-14 (1967), 1127.
- 7) J. Claus, IEEE Trans.Nucl.Sci. NS-20 (1973) 590.
- 8) J.J. Manca and H.R. Froelich, Nucl=Instr. and Meth. 136 (1976), 249.

